Analysis of the Pressure Variation Phenomena During Condensation Oscillation and Chugging

J. Prij, J.H.J. Seeverens

Netherlands Energy Research Foundation (ECN), P.O. Box 1, NL-1755 ZG Petten, The Netherlands

Abstract

To get a better understanding of the condensation oscillation and chugging process during blowdown of a BWR after a LOCA a large number of large scale pressure suppression experiments have been performed in several countries. ECN has performed a detailed analysis of the results of one of these experiments, e.g. the DAS M10 experiment of GKSS [1]. This analysis includes the following aspects: Power Spectral Density (PSD) analysis of the data, analysis of the acoustic frequencies of the downcomers and an analysis of the eigenfrequencies of the downcomers.

The results of these analyses and an evaluation are given in this paper. It is shown that all dominant frequencies in the experimental results can be correlated with the vent-acoustic or eigenfrequencies.

1. Introduction

The GKSS-test facility is a three pipe large scale vent system modeling main features of both the West German KWU type 69 and the United States MKII pressure suppression containment. The test facility is equiped with about 200 measurement sensors for registration of pressure, force, acceleration, mass flow, temperature and water level. The basic configuration of the test facility consists of a chain of four vessels: pressure vessel - drywell - wetwell - expansion room. The volumes of these vessels are respectively 22.5, 55.5, 114.6 and 58.6 m^3.

As can be seen in figure 1 drywell and wetwell are connected by three vent pipes, viz. pipe A, B and C. All the three pipes pass through the ceiling of the wetwell. Pipe A is connected to the upper part of the drywell, pipe B and C however are connected to the bottom of the drywell. More information about the test facility is given in [1] and [2].

2. Pressure history

The experiment starts with opening the gate valve in the connection pipe between drywell and pressure vessel. Immediately after opening this valve a shock wave enters the drywell and expands in the drywell atmosphere. This pressure increase, associated with the postulated LOCA, results in a compression wave in the water initially standing in the vent pipes. This water will accelerate into the pool, which results in a water jet. The pressure wave and the

water jet cause a pressure rise in the wetwell.

Immediately after the vent pipe clearing, a bubble of air starts to form at the exit of the vent pipes. When the air-steam flow from the drywell becomes established in the vent system, the initial bubble expands and subsequently decompresses as a result of overexpansion.

During the early stages of this process the pool will swell in bulk mode: a ligament of water is being accelerated upwards by the air bubble. As the water slub continues to rise, the pressure in the bubble falls below the pressure in the vent system. When the upward movement stops as a result of a decrease of the air-flow rate through the vent system, the gravity field and the increased pressure above the water, the "fall-back" process starts. During this process the pressure in the water will rise again. When a continuous steam flow begins pressure oscillation will occur (condensation oscillation). The static-pressure component will increase to a certain stationairy value. When the mass flow rate through the vent system decreases, the pool will begin to re-enter the vent pipes and the process of chugging starts. This period is characterized by sudden pressure pulses. In figs. 2, 3 and 4 a typical pressure-history of 3 locations of pipe B is given. Fig. 2 shows the pressure at the vent exit, fig. 3 at the steam front while fig. 4 presents the pressure at the bottom of the wetwell beneath the vent pipe.

Looking to the pressure-history diagrams of the pressure sensors at the exit of the pipes and "at the steam front" it can be seen that the pressure variations sketched in these figures follow the foregoing description, except at the very beginning of the experiment (the pressure rise as a result of the compression wave and the water jet is not registrated). The pressure variations at the steam fronts are much larger as those at the exits of the vent pipes. This can be explained by the fact that these sensors are periodically in the water region and the steam area. The pressure history diagrams of the sensors at the bottom of the wetwell shows no sudden decrease as a result of air bubble forming as could be expected.

The process of condensation oscillations starts about 12 seconds after the begin of the experiment. Chugging starts after about 100 seconds.

3. PSD analysis

The Power Spectral Density (PSD) analysis is carried out using the software packages HTR and PSD [3]. The data to be analysed are divided into a number of segments, each containing data which can be regarded as stationary. The program HTR determines for each block the model parameters (viz. the autoregression coefficients) by least square fit using Householder transformation. Using these autoregression coefficients the PSD values are calculated by the program for each segment of data. From these the average values of the PSD is calculated for the whole time interval. The PSD analysis is performed for two time series, viz.:

- From 45 s to 79.6 s. This time interval contains the process of condensation oscillation (CO).
- From 135 s to 169.6 s. This time interval contains the process of chugging.

The results for the time interval containing CO are given in fig. 5 for the three pressure sensors belonging to pipe B. In fig. 6 a comparison is given for the PSD Spectrum during CO and chugging.

4. Calculation of the vent acoustics

The natural frequencies of the steam venting system are calculated under the assumption that the steam is governed by linear acoustics, which means that the steam is treated as an isotropic, inviscid and irrotational medium and the velocity of the steam is small compared with the acoustic speed. Furthermore the gravity field is ignored. The fluid field is then described by [4]:

$$\nabla^2\varphi = \frac{1}{a^2}\frac{\partial^2\varphi}{\partial t^2} \qquad \bar{u} = \nabla\varphi \qquad p = -\rho_o\left(\frac{\partial\varphi}{\partial t}\right) = a^2\rho \tag{1}$$

where φ represents the velocity potential function, $\bar{u}$ the velocity vector, a the acoustic speed in the fluid, p the pressure, ρ_o the mass density of the fluid at rest, ρ the mass density of the pertubed fluid and a the acoustic speed (489 m/s).

If the velocity is one dimensional and sinusoidal, the general solution of equation (1) is given by:

$$\varphi = (R\cos k\xi + S\sin k\xi)\, e^{i\omega t} \text{ and } u = -k\,(-S\cos k\xi + R\sin k\xi)\, e^{i\omega t} \tag{2}$$

where ω is the circular frequency, k the wave number ($= \omega/a$), ξ the coordinate along the local axis and R and S are invariant.

The acoustic circuit used in this analysis is assumed to be one dimensional and the air-bubble beneath the exit of the pipe during the experiment is schematized as a cylinder with variable length. The continuity of pressure and velocity leads to a system of homogeneous equations. A nontrivial solution exists if the determinant of the coefficients vanishes. By means of an iterative computer code the values of $k = \frac{2\pi}{a} f$, for which the determinant vanishes, have been calculated. This is done for f = .5 Hz to 60 Hz with a stepsize of .05 Hz. The results of the analyses for some discrete values of the length of the airbubble are given in table I for pipe A and in table II for pipe B and C.

5. Calculation of the eigenfrequencies of the vent pipes

The eigenfrequencies of the vent pipes are calculated using the finite element code NASTRAN, version 63A [5]. The vent pipes are modelled by simple beam elements. The element properties are chosen according to the geometry of the pipes. The pipes are connected with flanges to the different vessels. Between these flanges and pipes, sealings are mounted and so the connection can neither be considered to be completely fixed nor be regarded as a simply support. To investigate the influence of the boundary conditions both extremes are analysed. The average submergence depth of the pipes in the water is about 1.1 m. The water will support the pipes to a certain degree. This influence is taken into account by adding a non-structural mass to the elements below water level. This is done with three different values of the non-structural mass, viz. 148, 292 and 438 kg/m. These values correspond with 0.5, 1 and 1.5 times the water mass which the pipes can contain per meter length. Chosen material constants: $E = 2.1 * 10^5$ MPa and $\nu = .3$. The analysis is performed using the modified Givens method to solve the eigenvalue problem as this method gives a high accuracy to the lowest calculated eigenfrequencies.

The results of the analyses upto 60 Hz are given in table III. It should be noted that the highest calculated eigenfrequency of vent pipe A, 48.2 Hz, belongs to an eigenfrequency of the upper part of the pipe, which explains the independency of this eigenfrequency to the value of the non-structural mass.

6. Evaluation and conclusions

The results of the pressure measurements and those of the frequency analysis have been presented in the preceding chapters.

From the time history plots presented in chapter two it can be seen that after the initial phase the pressure at the bottom of the wetwell is almost constant and at a pressure of .23 MPa. In order to compare the acoustic- and structural eigenfrequencies with the peak frequencies resulting from the PSD-analysis the results are presented in figs. 7 and 8 for the condensation oscillation process. The results for pipe C are almost equivalent with pipe B.

There is no significant difference between the frequencies during condensation oscillation and chugging. The following observations can be made now:

(1) All dominant frequencies of the pressure sensors in the direct surroundings of the ends of the vent pipes correspond to the different acoustic frequencies of the three vent pipes. In the pressure sensors of vents B and C there is also a dominant frequency of about 33 Hz which can be correlated with a vent acoustic of pipe A through reflections in the drywell.

(2) The frequency analysis of the pressure at the bottom of the tank below the vent pipes shows dominant frequencies corresponding to all vent acoustic and eigenfrequencies of the vent pipes. With respect to the lowest vent acoustic of 13 and 18 Hz of vent A and B, C respectively, it can be observed further that the PSD at 13 Hz is the highest for the pressure sensors below vent pipe A while the PSD at 18 Hz is the highest for the pressure sensors below pipes B and C.

(3) The PSD of the pressure sensors in the vent pipes is lower than the PSD of the pressure sensors in the water or on the wall of the tank.

(4) The PSD at a frequency corresponding to an acoustic frequency is higher than the PSD at a frequency corresponding to an eigenfrequency.

(5) The PSD at a lower vent acoustic is somewhat higher than the PSD at a higher acoustic frequency.

Based on these observations the following conclusions can be drawn.

(A) The pressure history during condensation oscillation is almost stationary while the small pressure oscillations are dominated by the acoustic frequencies of the vent pipes.

(B) All dominant frequencies in the pressure history during condensation oscillation correspond to acoustic frequencies or eigenfrequencies of the vent pipes.

(C) The highly dynamic processes of condensation oscillation and chugging do not have a dominant frequency in the range .5 - 60 Hz. All acoustic and eigenfrequencies of the system are reflected in the pressure response.

(D) The design of the pressure suppression system should be made such that vent acoustics and eigenfrequencies do not coincide.

7. References

[1] E. Aust, H.D. Fürst, H.R. Niemann, P. Sattler, J. Vollbrandt, DAS-Experimente der GKSS-Bericht über den Hauptversuch M10 GKSS 83/I/33, Mai 1983.

[2] E. Aust, H.D. Fürst, H.R. Niemann, Basisprogram über experimentelle Untersuchungen an Ein- und Mehrrohranordnungen für Druckabbausysteme von Kernkraftanlagen - Beschreibung der Druckabbau-Versuchstandes der GKSS. GKSS 79/E/8. Januar 1979.

[3] A.Th. Overtoom, N. Kitamura, E. Türkcan, Operating Manual of HTR and PSD "Programs for Spectral Density Analysis of Non-stationary Time Series Data Based on Least Squares Modeling", ECN 84-04, 1984.

[4] L.E. Kinsler, A.R. Trey, Fundamental of acoustics, John Wiley & Sons, New York, 1962.

[5] MSC/NASTRAN, version 63A, Users Manual, The MacNeal-Schwendler Corporation, Los Angeles.

[6] J. Prij, J.H.J. Seeverens, E. Türkcan, Analysis of the pressure variations during condensation oscillation and chugging in the GKSS Experiment M10. To be published as ECN report, 1985.

Table I: Vent acoustics pipe A (Hz)

Nr.	"length" airbubble (mm)			
	0	200	400	600
1	13.0	12.8	12.6	12.3
2	30.2	29.8	29.4	29.0
3	52.7	51.7	50.7	49.6

Table II: Vent acoustics pipe B/C (Hz)

Nr.	"length" airbubble (mm)			
	0	200	400	600
1	18.5	18.0	17.5	17.0
2	54.4	52.8	52.0	50

Table III: Eigenfrequencies of the vent pipes

VENT PIPE	SUPPORT	NON-STRUCTURAL MASS (kg/m)		
		146	292	438
A	simply support	7.8 8.2 48.2	6.5 6.8 48.2	5.7 6.0 48.2
	fixed	12.1	10.3	8.9
B/C	simply support	10.6	8.4	7.3
	fixed	12.1	10.3	8.9

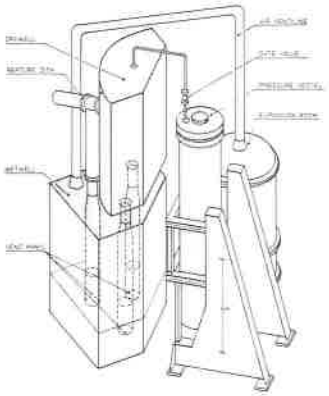

FIG 1 GENERAL ARRANGEMENT OF THE GKSS PSS-TEST FACILITY

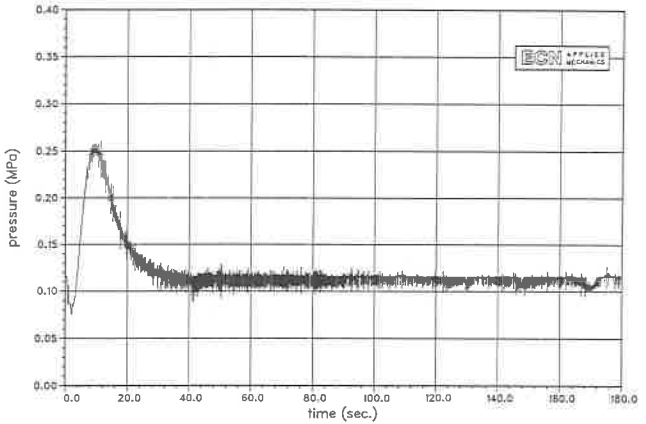

fig. 2. Pressure history channel KC–PG32

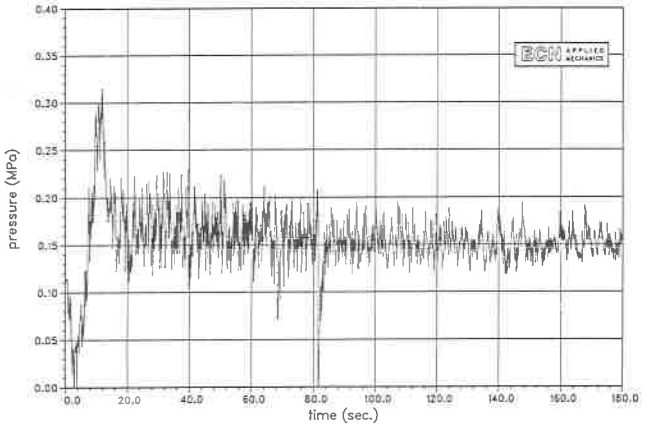

fig. 3. Pressure history channel WW–PG83

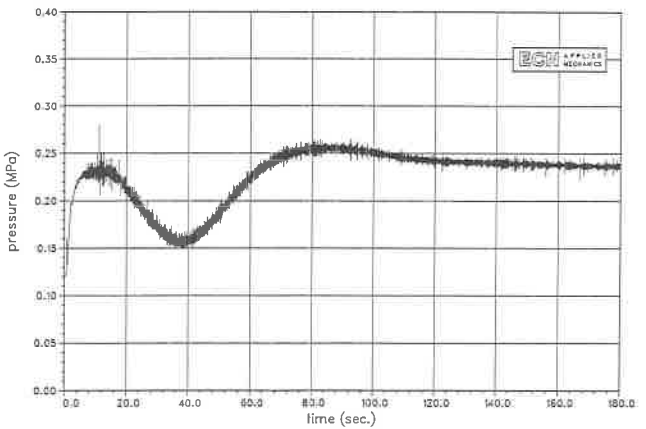

fig. 4. Pressure history channel WW–PA50

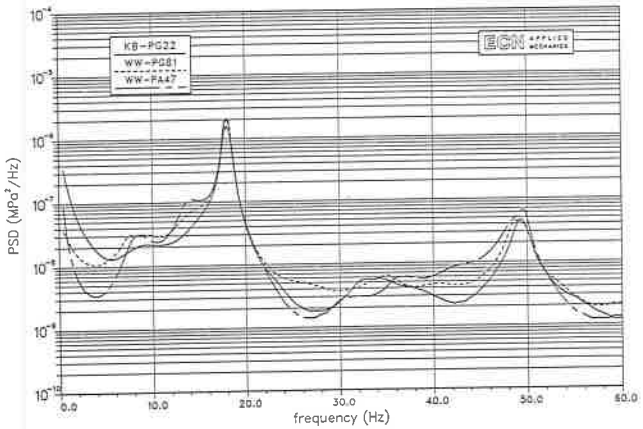

fig. 5. PSD spectrum vent pipe B during condensation oscillation

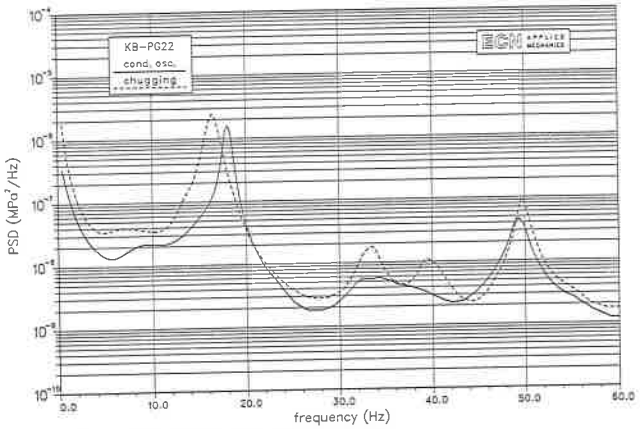

fig. 6. PSD spectrum at the exit of vent pipe B during condensation oscillation and chugging

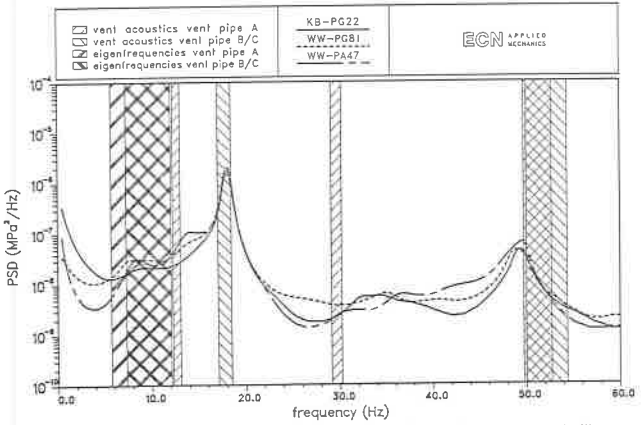

fig. 8. PSD spectrum vent pipe B during condensation oscillation compared with vent acoustics and structural eigenfrequencies of the vent pipes

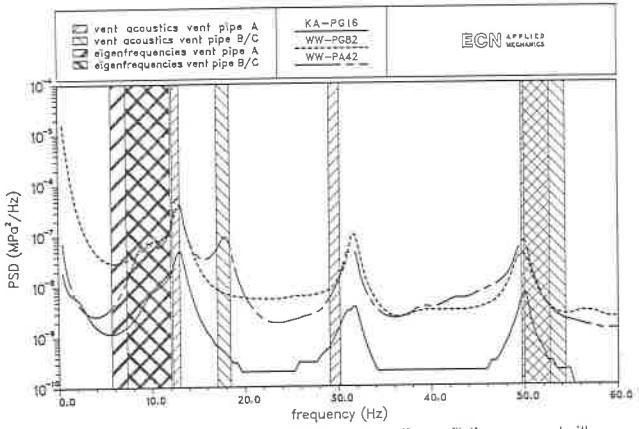

fig. 7. PSD spectrum vent pipe A during condensation oscillation compared with vent acoustics and structural eigenfrequencies of the vent pipes